

Convergence zone development in complex terrain during the Convective and Orographically-induced Precipitation Study (COPS)

Tracy Hertneky¹ and Tammy M. Weckwerth¹

¹*National Center for Atmospheric Research*
(5 September 2014)

Abstract

Clear-air atmospheric boundary-layer convergence zones are difficult to detect and study, especially in regions of complex terrain. These terrain-induced convergence boundaries can create favorable regions for convection initiation (CI) to occur and therefore it is important to understand where, when and how the boundaries will develop. During the Convective and Orographically-induced Precipitation Study (COPS), two Doppler On Wheels (DOW) mobile radars observed a variety of convergence boundaries in the Rhine River Valley and along the slopes of the Vosges and Black Forest Mountains in southwestern Germany and eastern France during the summer of 2007.

DOW reflectivity and radial velocities were manually examined for each of the 37 operational days. Of those days, only the terrain-induced boundaries with weak synoptic forcing are examined for this research study. Of the DOW operational days, 14 matched these criteria with half containing radar-observed boundaries either within the valley or along the lee slopes and the rest having no observed boundaries. By calculating the Froude value for each of these days, it was found that boundary days had a value larger than 1 while the non-boundary days had a calculated value less than one. The location of observed and model convergence zones correlated well and matched the conceptual model of the Froude number given in previous studies. Data from the DOWs, soundings and the Vienna Enhanced Resolution Analysis (VERA) surface data are combined to further understand boundary development, which is believed to depend strongly on the characteristic wind flow through and around the mountains, as well as stability within the valley. Additionally, model runs using the Weather Research and Forecasting (WRF) model have shown promise in replicating areas of convergence similar to those observed, and can therefore assist in filling in observational gaps. The focus of this research is to determine primary factors which lead to the development of these observed terrain-induced boundaries.

1. Introduction

It is difficult to observe the variability of ambient atmospheric conditions within complex mountain terrain. Adequate measurements within these regions are difficult due to atmospheric variability, limitations of instruments, and accessibility. Terrain-induced convergence boundaries are of particular importance in these regions, but are generally undetected for reasons such as lack of high resolution data coverage and radar beam blockage by the terrain. The importance of these convergence boundaries has long been documented to produce favorable locations for deep, moist convection initiation and therefore can play a major role in forecasting when and

where storms will form. Although not within a mountainous region, one of the first studies to associate low-level wind convergence to the initiation of thunderstorms was presented by Byers and Rodebush (1948) and Byers and Braham (1949). They determined that the anemometer-observed convergence caused by seabreezes along the Florida peninsula were the mechanism leading to daily afternoon thunderstorms in that region. Later studies began associating wind convergence to storm formation in complex terrain. In regions such as the Rocky Mountains, Wilson and Schreiber (1986) and Schreiber-Abshire and Rodi (1991) used a combination of radar and a surface mesonet network to identify boundary layer convergence lines in the region directly east of the north-south oriented mountain range. Lines were identified in Doppler radar fields as fine lines of enhanced reflectivity coupled with strong radial or azimuthal gradients in velocity. Boundary types found in their study included gust fronts and synoptic fronts as well as terrain-induced boundaries such as mountain outflow and Denver convergence lines. They found that 79% of the storms developing in their study region initiated near a convergence boundary. Banta and Schaaf (1987) looked at storm initiations within the Rocky Mountains and discovered preferred genesis locations related to convergence zones and that these genesis zones differed depending on the flow regimes. For example under westerly flow, the genesis zones were generally in the lee of the slopes but under northwesterly or southwesterly flow, these genesis zones occurred in a more southern lee or northern lee zone, respectively. In the mountain regions of western Washington state, Mass (1981) examined low-level convergence zone events in Puget Sound formed by the topographic configuration. The Puget Sound convergence zone develops when the coastal winds from the northwest flow around the Olympic Mountains and are forced to converge in the Sound by the north-south oriented Cascade Mountains resulting in a band of enhanced cloudiness and precipitation. This convergence zone undergoes a strong annual and diurnal cycle with it being most prominent in the afternoon/late evening of the early spring/summer months.

The Vertical Exchange and Orography (VERTIKATOR) project was conducted in the same region as COPS and showed that the area was frequented by enhanced convection (Barthlott et al., 2006). In this region, differential heating of the slopes and free atmosphere at the same height often leads to thermally-induced secondary circulations during the daytime. Favorable conditions for these systems to evolve include weak surface pressure gradients and clear skies. These wind systems then lead to mass and moisture convergence over elevated terrain, triggering the initiation of convection or enhancement of storms advecting over the area. He further used the Lokal Modell (LM) of the Deutscher Wetterdienst (DWD) to determine if the model was capable of reproducing such wind systems. While the 7-km resolution simulations region did not show these wind regimes, a smaller resolution at 2.8 km provided good agreement with near-surface winds and timing of CI, with the location being slightly off. A 9-year radar climatology of convective initiations and enhancements over the COPS region was conducted by Weckwerth et al. (2011), which concluded that the density of initiations over the mountains were twice as much as over the valley regions. It was also clear that the storms developing over the terrain became larger and stronger than those over the valley. A strong midday peak of these events suggest that they are produced by the aforementioned slope circulations and convergence boundaries caused by differential heating. Furthermore, the multitude of CI events in the valley led to the hypothesis that undetected boundary layer convergence zones frequently occur in region and may be the cause of the many CI events. The study of convergence boundary

formation and evolution can be used to produce improved forecasts of when and where convection is most likely to appear in these mountain and valley regions.

During the COPS field project, several cases involving convergence boundaries were studied. Hagen et al. (2011) studied the relationship of wind flow patterns around/through the Vosges Mountains and the location of low-level convergence and subsequent CI. Days with weak winds varying with height resulted in the flow being diverted around the terrain allowing for thermally-driven circulations leading to convergence and initiation on the ridge. However, when the flow was stronger and increasing with height, winds passed over the mountains or through the valley's leading to wind convergence and initiation on the lee side of the Vosges. Weckwerth et al. (2014) looked at the formation of deep convection on 6 August in the lee of the Vosges due to easterly upslope flow converging with the westerly ridge-top flow descending over the peaks. Moist convection was allowed due to the moistening of the region caused by the advance of a synoptic frontal system, surface evaporation, thermal convection and mixing. The case day of 15 July during the COPS campaign, which involved a convergence zone leading to deep convection, was studied in depth (Barthlott et al. 2010, Kalthoff et al. 2009, Richard et al. 2011). On this day, two convergence zones were observed. The first was related to a mesoscale convergence zone which approached the COPS region from the west. The second was a thermally-driven convergence zone which formed on the ridges of the Black Forest Mountains. Once the synoptically-induced mesoscale convergence zone became superimposed with the thermally-driven convergence zone, strong updrafts leading to deep convection were observed. In this case, moisture was transported to the ridge via slope circulations as well as from latent heat transformation due to cloud-free conditions and high insolation.

While many studies have examined convergence boundaries in various regions, they have not focused on the less understood terrain-induced boundaries which form due to slope and valley convergence. These types of boundaries remain undetected by operational radar due to their proximity within complex terrain, but are important because they play a role in mountain convection initiation. This study identifies such boundaries using radar data and evaluates possible mechanisms leading to formation using gridded surface data, soundings and Froude calculations. Further, it looks at convergence fields from model simulations to determine model capabilities of producing such terrain-induced boundaries.

2. COPS Convergence Boundary Analyses

2.1. Overview

In the summer of 2007, an international field campaign known as the Convective and Orographically-induced Precipitation Study (COPS) was conducted in the low mountain regions of southwestern Germany and Eastern France (Wulfmeyer et al. 2008, 2011). The study was designed to collect high-quality data to improve model representation of Quantitative Precipitation Forecast (QPF) over regions of complex terrain which proves to be a great challenge. The region included the Vosges and Black Forest Mountains with the Rhine Valley in between (Fig. 1) where it is common for severe thunderstorm activity to result in flash flood events.

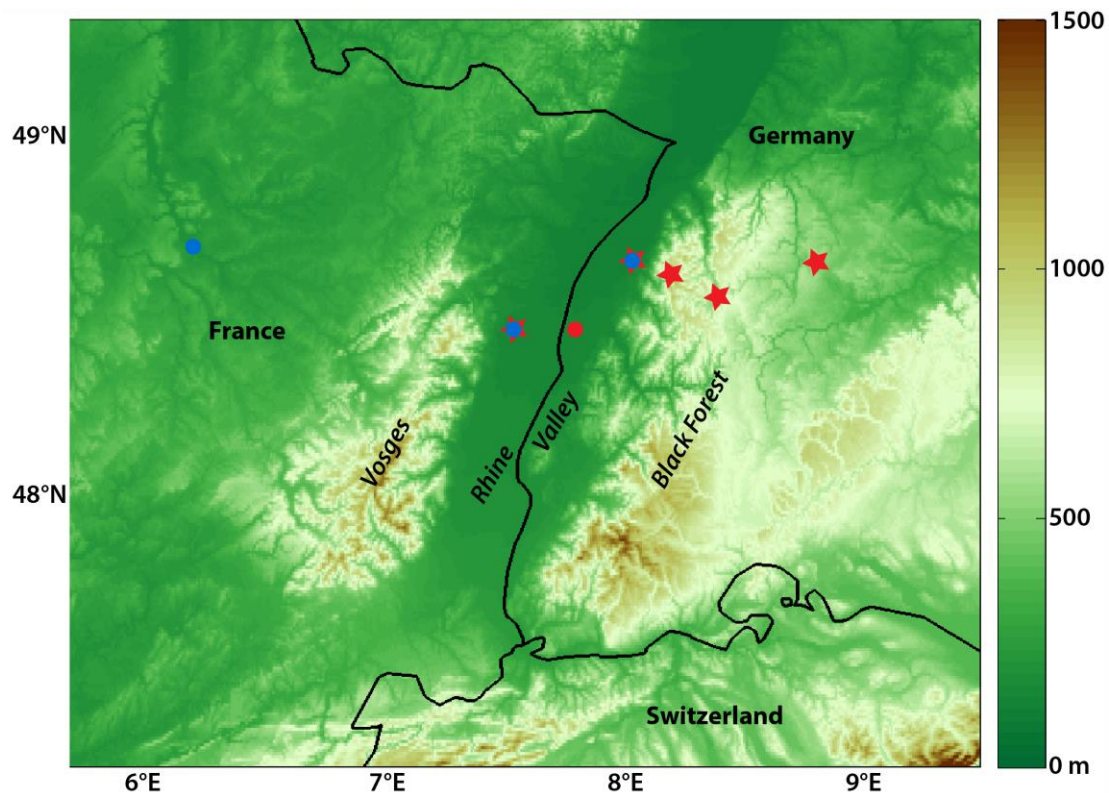


Figure 1. The domain of the COPS region is shown with colored terrain contours. The red stars are supersite locations, red dots are DOW sites, and blue dots are sounding locations.

During the COPS field campaign, two DOW radars operated a total of 37 days and 3 overnight periods. Each of these days were analyzed to determine the location, orientation, timing and approximate strength of any convergence boundaries. For this study, only the daytime periods were analyzed since there were very few night cases and possibly different mechanisms producing boundaries. A total of 24 boundaries were identified on 15 days and included frontal boundaries, outflow boundaries, and terrain-induced (including upslope) boundaries. However, only days with no significant large-scale dynamic forcing were included in order to focus on the local effects, such as slope and valley winds, resulting in boundary formation. For each of the operational days, 14 of them matched these criteria, with 7 containing some form of convergence and 7 with no convergence (see Table 1). The days without observed boundaries are also included in the study to compare differences of boundary versus non-boundary days. The convergence boundaries observed on the weak synoptic days consisted mostly of upslope boundaries along the Vosges or Black Forest Mountains, as well as a couple days with cross-valley terrain induced boundaries. For each boundary, the timing, location and orientation was recorded, however, start and end times of boundary formation were not possible for every day due to the radars not continually operating. In many cases boundaries were already present at the start of operations or they persisted after the radars were shut down for the day. The four days of upslope convergence did not exhibit any form of convection across the boundaries, but of the two boundaries in the valley, one of them did initiate convection. Further research will be conducted to examine the differences between these two boundaries which formed in similar locations with one generating cells while the other did not. This paper will focus on comparing and contrasting one boundary day (25 July) and one non-boundary day (13 July) to reveal differences in environmental conditions leading to boundary formation.

Table 1. 14 days with weak synoptic forcing are listed and include the type of boundary observed, synoptic weather patterns, below ridge-top wind speeds and direction from the GFS at 1200 UTC and the Froude value. Boundary days are highlighted in green while non-boundary days are highlighted in blue. The wind and Froude values for 14 August were calculated from the Nancy sounding since GFS data was not available on that day.

	Boundary Type	Synoptic Features	Wind Speed	Wind Direction	Froude Value
19 June	none	500mb ridge No fronts	4.0	92	0.63
24 June	upslope	Weak Ridge – transition zone No fronts	5.6	188	1.36
30 June	Valley	500mb ridge No fronts	4.5	221	1.16
13 July	none	500mb ridge No fronts	4.4	178	0.66
14 July	upslope	500mb ridge – transition zone No fronts	6.0	205	0.85
15 July	upslope	500mb ridge – transition zone No fronts	13.3	195	1.70
16 July	upslope	500mb ridge – transition zone No Fronts	8.1	193	1.48
18 July	none	Transition zone Stationary front nearby	3.1	219	0.68
19 July	none	Transition zone No fronts	1.5	270	0.20
25 July	Valley	500mb ridge No fronts	3.8	246	1.20
26 July	upslope	Transition zone No fronts	7.4	212	2.20
4 August	None	500mb ridge No fronts	4.0	75	0.58
12 August	none	Transition zone Cold front nearby	0.5	175	0.11
14 August	none	Transition zone No fronts	4.1	210	0.76

2.2 Observational Analysis

2.2.1. Synoptic Discussion

As previously stated, the 14 days presented in this study exhibited weak synoptic forcing with no frontal influence and no observed precipitation at the radars. For these cases, the COPS domain was generally located under a 500mb ridge or just entering into a transition zone from a ridge where the forcing was still considered weak. Figures 2, 3 and 4 illustrate the synoptic conditions at 1200 UTC observed for the 25 July and 13 July cases. For the 25 July case, a low

pressure center is observed over the north Atlantic (Fig. 2a) with a surface cold front reaching out along the western European coast line (Fig. 3a). Another low pressure is seen over northeastern Europe, while the COPS region is located within the ridge in between the two lows. The non-boundary day on 13 July exhibits a similar pattern with a low pressure center located over the north Atlantic and another over northeastern Europe, with the COPS region under a ridge influencing central Europe (Fig. 2b). A surface cold front extends south from Ireland and a warm front reaches to the east into northern Germany (Fig. 3b). On both days the COPS region is influenced by high surface pressure. The synoptic patterns exhibited by these two cases, as well as the others listed in Table 1, support strong surface heating with weak synoptic forcing and clear skies, which generally results in strong diurnal valley wind systems. While seven of the cases did result in the formation of boundaries, boundaries were not observed in the radar for the other days under similar synoptic conditions.

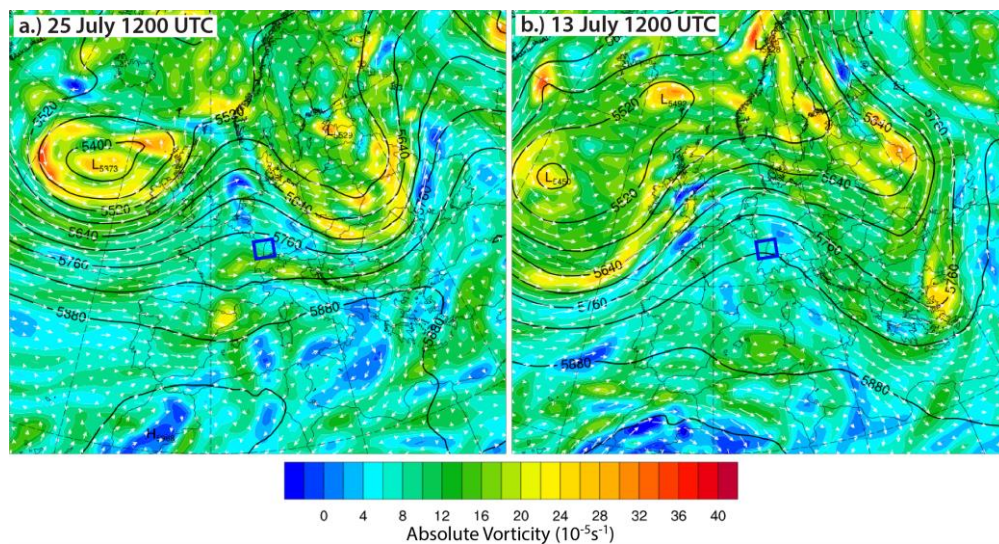


Figure 2. The maps show 1200 UTC 500mb GFS analyses with heights contoured in black and color contours of absolute vorticity for the 25 July boundary case (a) and the 13 July non-boundary case (b). The COPS region is identified as the blue box.

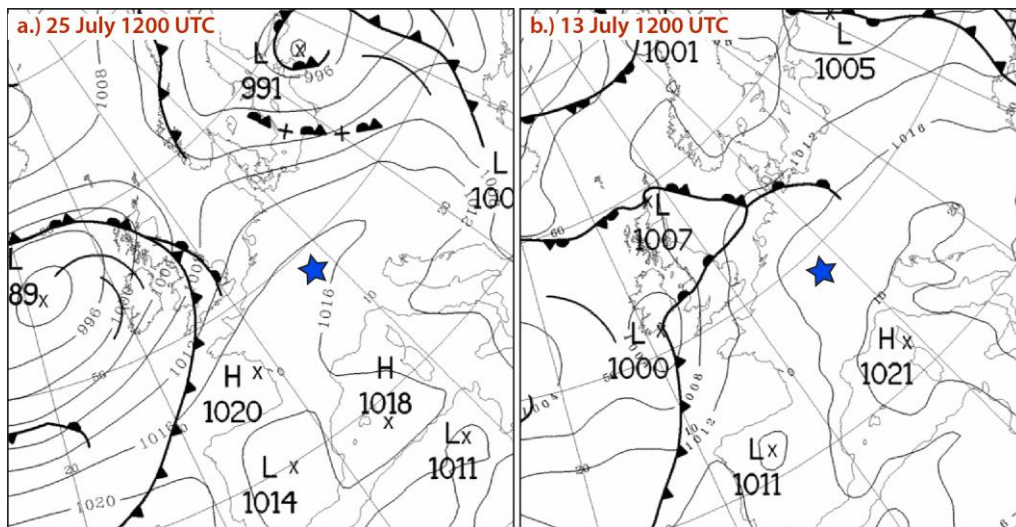


Figure 3. Surface plots for 1200 UTC show surface pressure contours and surface fronts for the 25 July boundary case (a) and the 13 July non-boundary case (b). The COPS region is indicated by a blue star. Courtesy of the UK Met Office.

2.2.2. Satellite

High-resolution visible satellite imagery taken from the Meteosat Second Generation (MSG) satellite show clear skies on both mornings, with small cumulus forming during the day time periods. Figure 4 shows the satellite image at 1200 UTC (UTC = central European summer time (CEST) - 2 h) for both days over the COPS region. On the 25 July boundary day, the number of cumulus forming is more numerous and covers a larger area including the mountain slopes and Rhine Valley. At 0900 UTC, the convection initiation which is observed to form along the boundary on 25 July is apparent on the western side of the valley and growing as it moves over the valley and then dissipating at 1200 UTC as it reaches the northern Black Forest Mountains (not shown). On 13 July, far fewer cumulus are observed and formation is limited to the ridge tops of the Vosges and Black Forest Mountains.

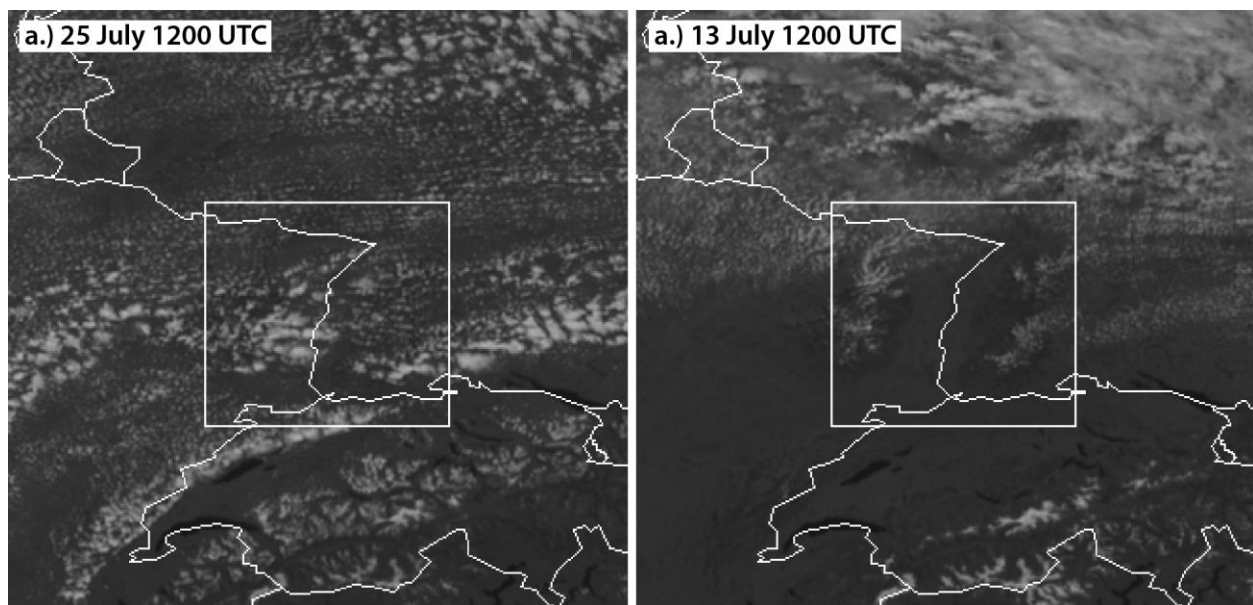


Figure 4. High-resolution visible satellite imagery from the Meteosat 2nd generation satellite for the 25 July boundary day (a) and the 13 July non-boundary day (b) at 1200 UTC. The white box indicates the COPS region.

2.2.3. Radar

During the COPS campaign, two Doppler on Wheels (DOW) radar were operating in various locations within the Rhine Valley and Black Forest Mountains. The DOWs are X-band (3 cm wavelength) radars with a beamwidth of 0.93° (Wurman et al., 1997). During operations, they used 150m gate spacing and a range of 50 km for most scans. Approximately 10 scanning angles were used ranging from 1.3° to 10° . Using the DOW radars, each day was manually analyzed to determine if a convergence boundary was present. A boundary was identified by looking at both the radial velocity field and the reflectivity field. Boundaries are typically observed as strong opposing winds flowing towards each other accompanied by a line of enhanced reflectivity at that location. For these two cases, the DOW radar was located in the northern Rhine Valley as indicated by a red circle in Fig. 1. On 25 July, DOW operations began just before 0900 UTC with southerly winds at the radar and a line of convergence already seen 15 km to the northwest in the valley within good clear air return. At 0920 UTC two cells form

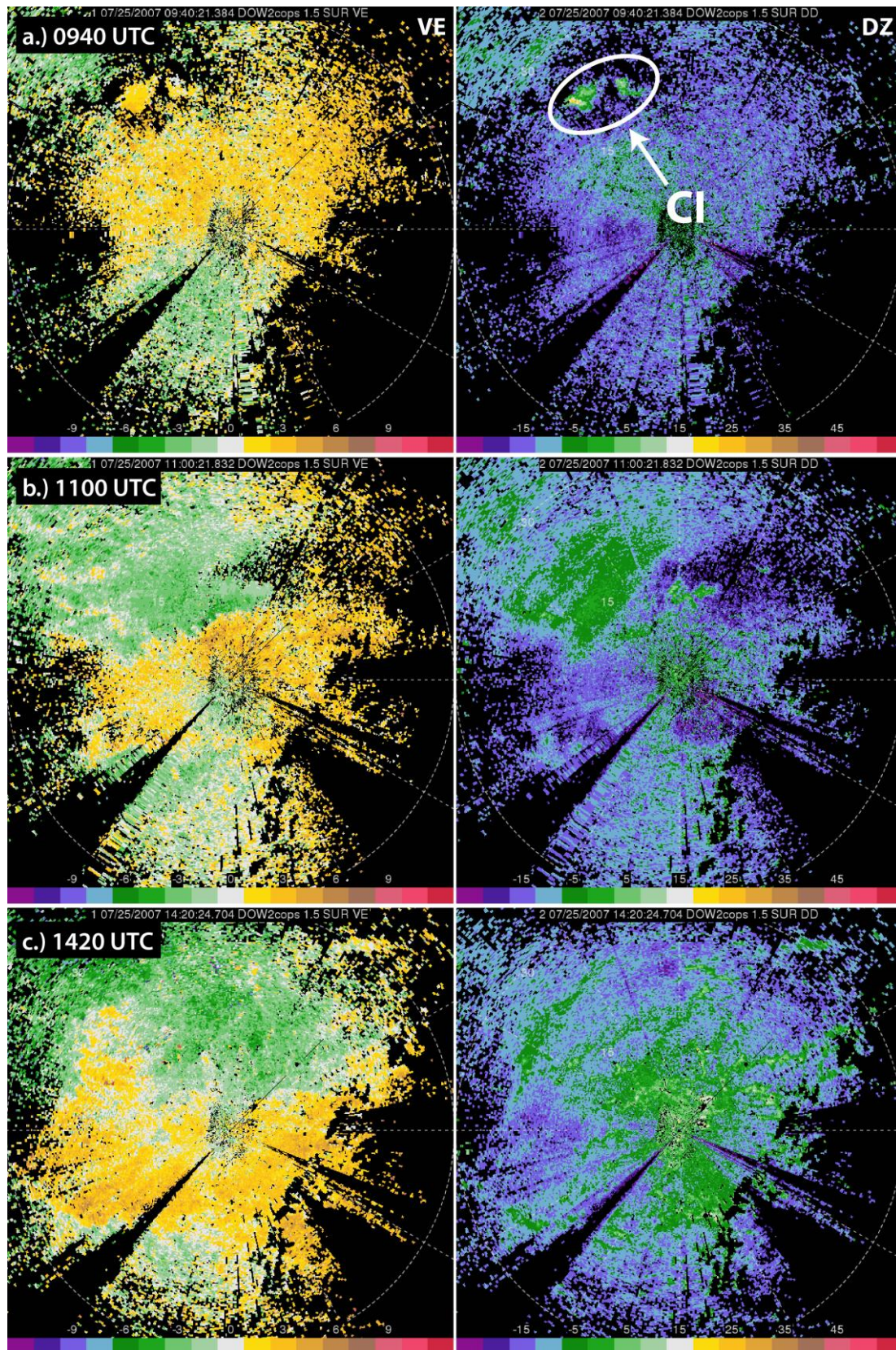


Figure 5. DOW radial velocities (left panels) and reflectivities (right panels) at 1.5° elevation angle for a.) 0940 UTC b.) 1100 UTC and c.) 1420 UTC.

along the boundary. Fig. 5a shows these CI along the boundary at 0940 UTC after they have grown. The CI persists along the boundary with little growth and the small cells move eastward off the boundary where they dissipate by 1100 UTC. At this time the boundary has become stronger and more defined (Fig. 5b) and by 1300 UTC a second boundary south of the radar and oriented parallel to the first has developed. At 1420 UTC, the region of convergence has become complex with convergence observed to the north, west and south, however, no new convection is observed (Fig. 5c). Upslope is present in the lee of the Vosges with hints of upslope convergence; however, due to the limited amount of scatterers at that location, an obvious boundary is not identified until later in the day. Radar operations end around 1620 UTC on this day with convergence still present to the northwest. While the 13 July case exhibited upslope in both the Vosges and Black Forest Mountains, no defined convergence boundary lines along the slopes are observed (not shown). It is possible that with these days where boundaries are not observed in the radar, convergence could still be present along the ridge where the limited radar scans may not intersect.

2.2.4. VERA

The Vienna Enhanced Resolution Analysis (VERA) is a 2-dimensional gridded surface analysis covering Central Europe (Steinacker et al., 2000). It uses the irregularly spaced Global Telecommunication System (GTS) and non-GTS surface station data set, which provides fields such as wind, temperature, mixing ratio, and precipitation every hour. The method combines prior knowledge about thermal and dynamical atmospheric behavior due to topographic forcing along with station measurements to produce 8-km gridded surface analyses. The fact that a numerical model or other first-guess field is not used makes it ideal for validation to numerical models. Obvious differences are seen in the VERA analysis when comparing the boundary and non-boundary case with winds seeming to be a major role in boundary development (Fig. 6). For the 25 July boundary case, winds in the valley start out southerly in the morning and become lighter and variable between the two mountain ranges as daytime heating and slope flows begin.

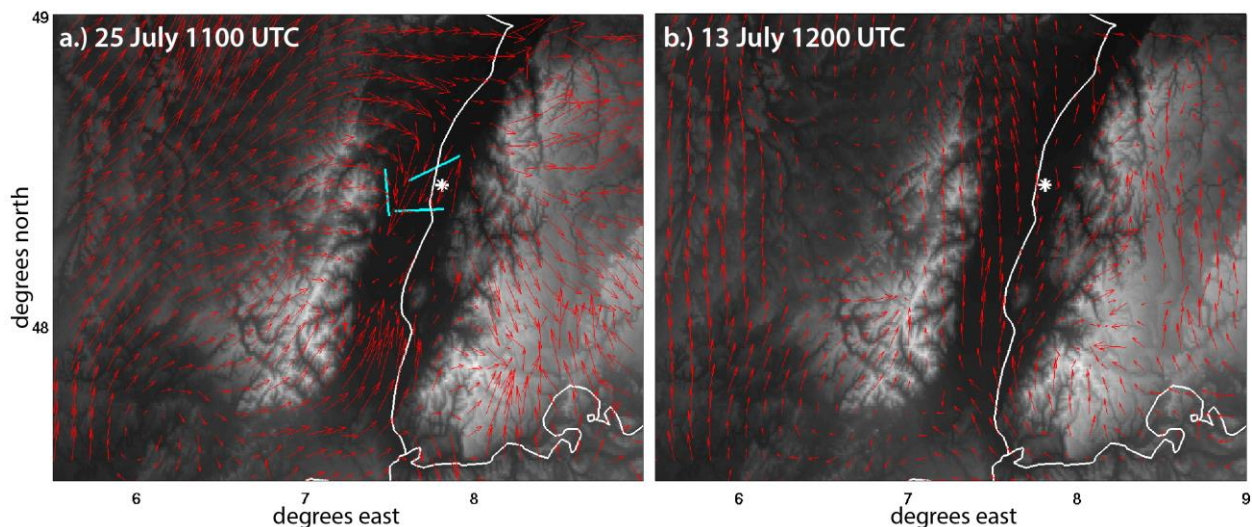


Figure 6. Surface winds from the VERA analysis with terrain contoured in grey-scale on 25 July 1100 UTC (a) with boundary locations plotted in cyan and the non-boundary case on 19 June 1200 UTC (b). DOW locations for each day are indicated by the white star(s).

Stronger winds continue to flow around the northern and southern Vosges where they collide with the stagnant air in valley creating favorable regions for convergence. The location of the converging surface winds in the northern Rhine matches nicely with the observed radar boundary locations (solid cyan lines) shown in Fig. 6a at 1100 UTC. At this time, westerly winds can also be seen colliding with the valley air in the lee of the Vosges which also matches with the location of upslope convergence hinted in the radial velocity field. On the other hand, winds are stronger on the 13 July non-boundary day and maintain a southerly direction in the valley. In this case slope and valley winds are not clearly observed; however, areas of converging winds are identified along the ridge tops of the Vosges and Black Forest mountains. While the surface moisture and temperatures are higher in the valley on the non-boundary day by around 2 g kg^{-1} and 5 K , respectively, the lack of organized convergence in the valley does not favor valley CI as is seen on the boundary day.

2.2.5. Froude Number and Stability

The Froude number was calculated in order to quantify the flow around the Vosges Mountains for each of the 14 weakly-forced days and is given by the equation

$$Fr = \frac{U}{NH},$$

where U is the average wind speed between 950-925 mb, N is the Brunt-Vaisala frequency between 975-850mb and H is the height of the mountain, in this case 800m. For this study, a profile about 100 km west of the Vosges Mountains taken from the GFS analysis at 1200 UTC was used to represent the upstream flow for the calculations. This data was used over a typical sounding due to the lack of soundings in the upstream region and because it contained a variety of vertical levels. The nearest sounding location was at Nancy, France to the northwest; however, since a majority of the days had westerly or southwesterly flow, it was less ideal for representing the upstream flow. The Nancy data also only included the required standard levels which were fewer than desired. Table 1 lists wind, stability and Froude values for each of the 14 days. When the Froude number is less than 1, the upstream low-level flow is blocked and instead flows around the mountain obstacle. For Froude numbers greater than 1, air is not blocked and will flow over the mountain as well as channel through the valleys. For the boundary days, the Froude value was generally greater than 1, with the exception of 14 July which is near 1 and also significantly higher than the non-boundary days. According to a study by Hagen et al. (2011), which included similar calculations of the Froude number for the same area, the flow on these days would pass over the mountains and through valleys where it would collide with weak or stagnant flow within the valley, resulting in lee-slope or valley convergence. Indeed, these are the locations of the DOW-observed convergence boundaries. Alternatively, the non-boundary days all had a Froude value less than 1 in which the flow is blocked and flows around the mountain. In these low Froude number cases, convergence would be seen on the ridge of the mountains due to thermally-driven slope winds. Ridge-top convergence, however, was not observed by the DOWs and it is possible that the limited elevation angles that the radars operated at were not frequent enough at higher elevations to observe such ridge-top convergence. Due to the fact that there appears to be such a strong relation to the Froude number and the formation of boundaries within the valley and lee slopes, this information could be valuable in forecasting their formation and possible subsequent CI along the boundary.

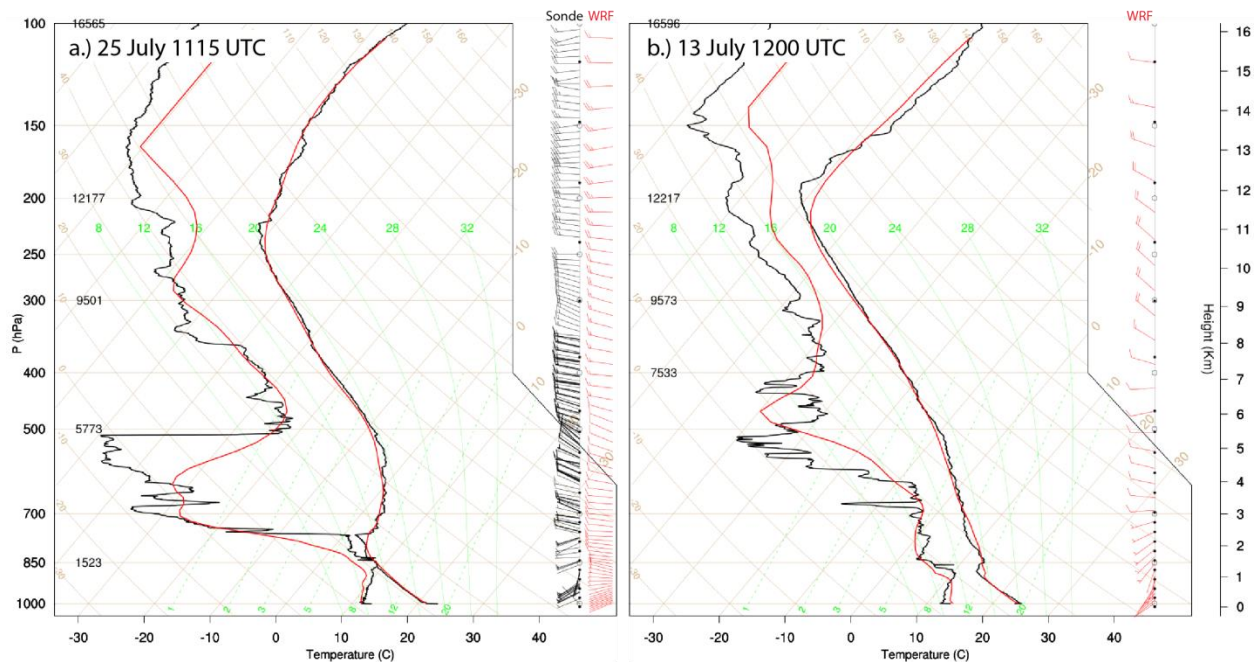


Figure 7. Soundings taken from the Achern site northwest of the radar for a.) 25 July non-boundary day at 1115 UTC and b.) 13 July non-boundary day at 1200 UTC. The solid black line is the observed sounding and the solid red line is the WRF profile at the location of the sounding. For 13 July the sounding winds were not retrieved.

Soundings are shown in Fig. 7 for 25 July 1115 UTC (Fig. 7a) and 13 July 1200 UTC (Fig. 7b) from the Achern site which is 28 km to the northwest of the radar (see Fig. 1). The sounding profiles (solid black line) and westerly winds are relatively similar for both of the cases with the boundary day exhibiting a moister and deeper boundary layer than the non-boundary day. On 25 July, a dry surface layer is topped by a 1 km deep moist layer above which a pronounced inversion is present at 2.5 km. Above 2.5 km resides a deep dry layer, further inhibiting strong convection. Radar observed CI remained small and was only seen to a maximum height of 2.5 km which can be explained by the moist, but shallow region of positive buoyancy in the profile. On 13 July, the dry surface layer was capped by an inversion at 1.4 km resulting in a much shallower boundary layer depth. That coupled with the dryness of the column could explain the lack of initiation along the ridge when looking at both the radar and satellite. While the differences in these two profiles cannot give any insight into why one day observes valley convergence and the other does not, it is instead helpful in determining if CI may form along observed convergence boundaries.

2.3. WRF Simulations

The Weather Research and Forecasting (WRF) model (Skamarock 2008) was run for both case days to determine if it was capable of replicating areas of organized convergence at the location where boundaries were observed, or not observed for the null cases. Simulations were run for 12 hours starting at 0600 UTC with a time resolution of 10 minutes and grid resolutions of 3 km and 1 km for the outer and inner domains, respectively. Physics packages included the Thompson microphysics (Thompson et al. 2004), Mellor-Yamada-Janjic boundary layer physics (Mellor and Yamada 1982; Janjic 1990, 1996, 2002) and the NOAH land-surface model (Chen and Dudhia 2001).

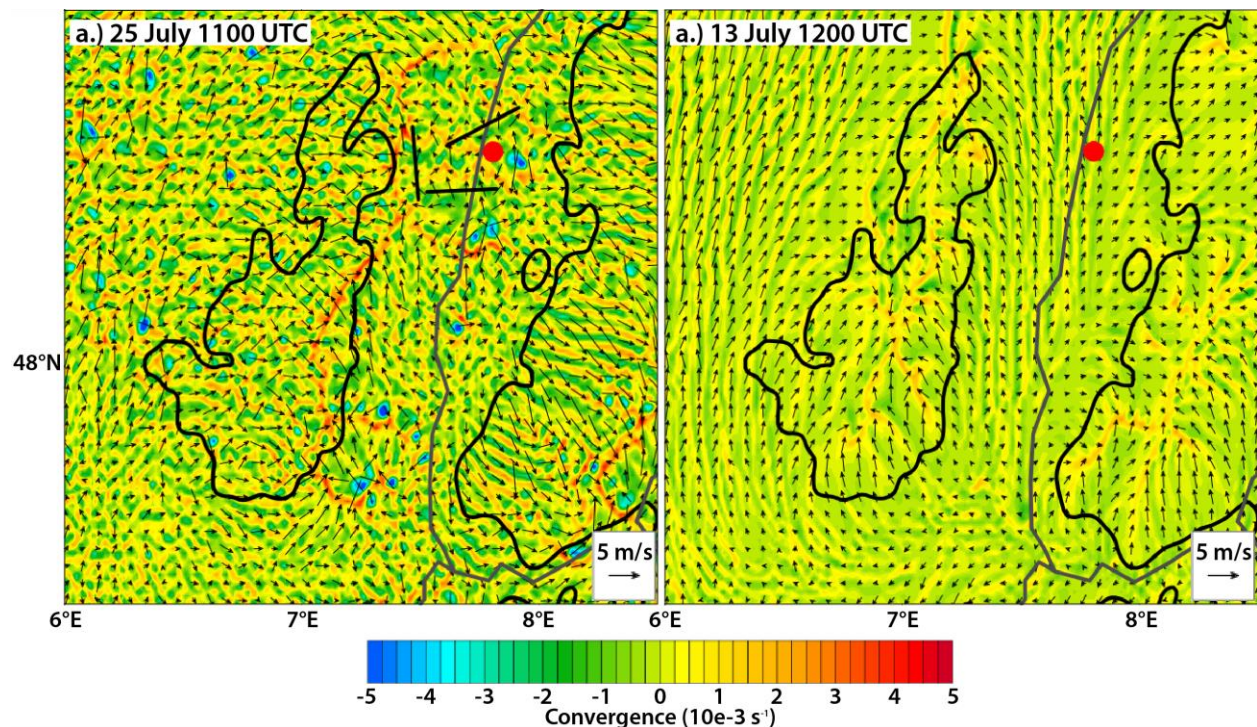


Figure 8. WRF simulations over the COPS domain for a.) 25 July boundary case and b.) 13 July non-boundary case. Colored contours are convergence at 10 m heights with 10 m wind vectors overlaid. The solid black lines are the locations of DOW-observed convergence boundaries and the red circle is the location of the DOW radar.

Simulations were run for both the boundary and non-boundary cases and results of the convergence and wind fields at 10 m height shown in Fig. 8. Notable differences are observed in the convergence field for the two cases. For the boundary case on 25 July (Fig. 8a.), lines of organized convection appear in the northern and southern Rhine Valley where winds were seen converging with the stagnant valley air in the observations. Upslope convergence is also observed along the length of the Vosges on the lee side. The location of the observed radar convergence boundaries are plotted as solid black lines and match relatively well with the WRF simulations relative to orientation and location. On the other hand, the non-boundary day on 13 July (Fig. 8b) exhibits no organized convergence within the Rhine Valley or in the lee of the Vosges. Instead, convergence boundaries are located along the ridge tops of the Vosges and Black Forest Mountains. It is quite possible that these boundaries were present on this day and were just undetected by the radar due to the limited elevation angles scanning at that height and distance from the radar. Further, the locations of the boundaries on each of the days correspond with the calculated Froude values and flow patterns discussed in previous studies (e.g., Hagen et al. 2011). For the 25 July boundary case, the Froude value from Table 1 was 1.2, in which case, the wind is expected to flow over the mountains and through valleys where it collides with the valley air. Indeed, both observations and WRF showed convergence in the valley and lee of the slopes. For the non-boundary case, the Froude value was lower at 0.66, in which the upstream winds are blocked and convergence is formed along the peaks through differential heating leading to thermally-induced slope winds. Again, the location of the convergence on this day corresponds well with this concept.

3. Conclusions

Clear-air boundary-layer convergence zones were observed in the Rhine Valley and adjacent slopes throughout the COPS campaign. The understanding and study of these boundaries are important because they often go undetected by operational radar but provide favorable locations for thunderstorms to develop in a region with already poor QPF skill due to complex terrain. This study focused on the less-understood terrain-induced boundaries observed under weak synoptic conditions where further analysis of the localized mechanisms leading to formation is warranted. Two case days, one with and one without convergence boundaries were picked for further evaluation.

On 25 July, convergence boundaries were observed to the north and south of the radar as winds flowed into the valley from the north and south, converging with the valley winds. Upslope convergence along the Vosges was also present, although difficult to detect due to poor scattering until later in the day. The locations of these boundaries matched the concept that when the Froude number was greater than 1, as seen on this day, winds would flow over the mountains and through the valleys where they would converge in the Rhine Valley and lee of the slopes. Further correlations were found when comparing to the WRF convergence field, which illustrated lines of organized convergence extending across the valley and along the lee of the Vosges in similar locations as observed. On this same day convection initiation developed along the northern boundary where converging winds and the presence of a moist layer above the LCL provide favorable conditions for CI. On the other hand, the capping inversion at 2.5 km likely prevented the convection from developing further. On the 13 July, no boundaries or CI were detected by the radar, but winds were observed converging along the ridges of the mountains in the VERA wind field. A Froude value of less than 1 on this day corresponds well with the concept that winds would be blocked by the mountain and convergence would form along the ridge-tops due to diurnal heating. The convergence field from WRF further supports this by also showing organized convergence lines along the ridges of the mountains.

The two studies examined thus far and which are presented in this study show that regions of convergence can be determined from high-resolution radar data and predicted by the Froude value and model simulations. This is an important step in forecasting where low-level boundaries and subsequent CI may occur within this region of complex terrain. Further analyses of additional boundary and non-boundary days are required in order to obtain a more robust conclusion.

Acknowledgement

Thank you to Greg Thompson for the advice and knowledge shared while working with the WRF model.

References

- Banta, R.M. and C.B. Schaaf, 1987: Thunderstorm genesis zones in the Colorado Rocky Mountains as determined by traceback of geosynchronous satellite images. *Mon. Wea. Rev.*, **115**, 463–476.
- Barthlott C., C. Corsmeier, C. Meißner, F. Braun, C. Kottmeier, 2006. The influence of mesoscale circulation systems on triggering convective cells over complex terrain. *Atmos. Res.* 81: 150–175.
- Barthlott C., J.W. Schipper, N. Kalthoff, B. Adler, A. Blyth, and S. Mobbs, 2010: Model representation of boundary-layer convergence triggering deep convection over complex terrain: A case study from COPS. *Atmos Res.*, 95: 172–185. DOI: 10.1016/j.atmosres.2009.09.010
- Byers, H.R. and H. R. Rodebush, 1948: Causes of thunderstorms of the Florida peninsula. *J. Meteor.*, **5**, 275–280. DOI: 10.1175/1520-0469(1948)005<0275:COTOTF>2.0.CO;2
- Byers, H.R. and R.R. Braham, Jr., 1949: *The Thunderstorm*. U.S. Govt. Printing Office, Washington, DC, 287 pp.
- Chen, F., and J. Dudhia, 2001: Coupling an advanced land-surface/ hydrology model with the Penn State/ NCAR MM5 modeling system. Part I: Model description and implementation. *Mon. Wea. Rev.*, **129**, 569–585.
- Hagen, M., J. van Baelen, and E. Richard, 2011, Influence of the wind profile on the initiation of convection in mountainous terrain. *Q.J.R. Meteorol. Soc.*, **137**: 224–235. doi: 10.1002/qj.784
- Janjic, Z. I., 1990: The step-mountain coordinate: physical package. *Mon. Wea. Rev.*, 118, 1429–1443.
- Janjic, Z. I., 1996: The surface layer in the NCEP Eta Model, *Eleventh Conference on Numerical Weather Prediction*, Norfolk, VA, 19–23 August; Amer. Meteor. Soc., Boston, MA, 354–355.
- Janjic, Z. I., 2002: Nonsingular Implementation of the Mellor–Yamada Level 2.5 Scheme in the NCEP Meso model, *NCEP Office Note*, No. 437, 61 pp.
- Kalthoff N., B. Adler, C. Barthlott, U. Corsmeier, S. Mobbs, S. Crewell, K. Traumner, C. Kottmeier, A. Weiser, V. Smith and P. Di Girolamo, 2009: The impact of convergence zones on the initiation of deep convection: A case study from COPS. *Atmos. Res.*, 93: 680–694. DOI: 10.1016/j.atmosres.2009.02.010
- Mass C., 1981: Topographically forced convergence in western Washington state. *Mon. Wea. Rev.*, **109**, 1335–1347. doi: 10.1175/1520-0493(1981)109<1335:TFCIWW>2.0.CO;2
- Mellor, G. L., and T. Yamada, 1982: Development of a turbulence closure model for geophysical fluid problems. *Rev. Geophys. Space Phys.*, **20**, 851–875.
- Richard, E., J. –P. Chaboureaud, C. Flamant, C. Champollion, M. Hagen, K. Schmidt, C. Kiemle, U. Corsmeier, C. Barthlott and P. Di Girolamo. 2011, Forecasting summer convection over the Black Forest: A case study from the Convective and Orographically-induced Precipitation Study (COPS) experiment. *Q.J.R. Meteorol. Soc.*, 137: 101–117. doi: 10.1002/qj.710

Schreiber-Abshire, W. and Rodi, A. R., 1991: Mesoscale convergence zone development in northeastern Colorado under southwest flow. *Mon. Wea. Rev.*, **119**, 2956–2977. doi: 10.1175/1520-0493(1991)119<2956:MCZDIN>2.0.CO;2

Skamarock W.C. and Coauthors, 2008: A description of the advanced research WRF version 3, NCAR Tech Note NCAR/TN-475+STR, pp 113. [Available online at http://www.mmm.ucar.edu/wrf/users/docs/arw_v3.pdf]

Steinacker, R., C. Häberli, and W. Pöttschacher, 2000: A transparent method for the analysis and quality evaluation of irregularly distributed and noisy observational data. *Mon. Wea. Rev.*, **128**, 2303–2316, doi:10.1175/1520-0493(2000)128<2303:ATMFTA>2.0.CO;2.

Weckwerth, T. M., J. W. Wilson, M. Hagen, T. J. Emerson, J. O. Pinto, D. L. Rife and L. Grebe. 2011, Radar climatology of the COPS region. *Q.J.R. Meteorol. Soc.*, 137: 31–41. doi: 10.1002/qj.747

Weckwerth T. M., L. J. Bennett, L. J. Miller, J. van Baelen, P. Di Girolamo, A. M. Blyth, and T. J. Hertneky, 2014: An Observational and Modeling Study of the Processes Leading to Deep, Moist Convection in Complex Terrain. *Mon. Wea. Rev.*, **142**, 2687–2708. doi: 10.1175/MWR-D-13-00216.1

Thompson, G., R. M. Rasmussen, and K. Manning, 2004: Explicit forecasts of winter precipitation using an improved bulk microphysics scheme. Part I: Description and sensitivity analysis. *Mon. Wea. Rev.*, **132**, 519–542.

Wilson J. and Schreiber W., 1986: Initiation of convective storms at radar-observed boundary-layer convergence lines. *Mon. Wea. Rev.*, **114**, 2516–2536. doi: 10.1175/1520-0493(1986)114<2516:IOCSAR>2.0.CO;2

Wulfmeyer, V., A. Behrendt, H.-S. Bauer, C. Kottmeier, U. Corsmeier, A. Blyth, G. Craig, U. Schumann, M. Hagen, S. Crewell, P. Di Girolamo, C. Flamant, M. Miller, A. Montani, S. Mobbs, E. Richard, M.W. Rotach, M. Arpagaus, H. Russchenberg, P. Schluskel, M. König, V. Gartner, R. Steinaker, M. Dorniger, D.D. Turner, T. Weckwerth, A. Hense, and C. Simmer, 2008: Research campaign: The convective and orographically induced precipitation study - A research and development project of the World Weather Research Program for improving quantitative precipitation forecasting in low-mountain regions. *Bull. Ame. Meteor. Soc.*, **89**, 1477-1486, DOI: 10.1175/2008BAMS2367.1.

Wulfmeyer, V., A. Behrendt, C. Kottmeier, U. Corsmeier, C. Barthlott, G. C. Craig, M. Hagen, D. Althausen, F. Aoshima, M. Arpagaus, H. –S. Bauer, L. Bennett, A. Blyth, C. Brandau, C. Champollion, S. Crewell, G. Dick, P. Di Girolamo, M. Dorninger, Y. Dufournet, R. Eigenmann, R. Engelmann, C. Flamant, T. Foken, T. Gorgas, M. Grzeschik, J. Handwerker, C. Hauck, H. Höller, W. Junkermann, N. Kalthoff, C. Kiemle, S. Klink, M. König, L. Krauss, C. N. Long, F. Madonna, S. Mobbs, B. Neiningen, S. Pal, G. Peters, G. Pigeon, E. Richard, M. W. Rotach, H. Russchenberg, T. Schwitalla, V. Smith, R. Steinacker, J. Trentmann, D. D. Turner, J. van Baelen, S. Vogt, H. Volkert, T. Weckwerth, H. Wernli, A. Wieser and M. Wirth. 2011, The Convective and Orographically-induced Precipitation Study (COPS): the scientific strategy, the field phase, and research highlights. *Q.J.R. Meteorol. Soc.*, 137: 3–30. doi: 10.1002/qj.752

Wurman, J., J. Straka, E. Rasmussen, M. Randall, and A. Zahrai, 1997: Design and deployment of a portable, pencil-beam, pulsed, 3-cm Doppler radar. *J. Atmos. Oceanic Technol.*, 14, 1502–1512, doi:10.1175/1520-0426(1997)014,1502:DADOAP.2.0.CO;2.